Simulations of *E.* coli adhesion under fluid flow.

By Juan Diego Arango-Montoya

Departamento de física

Universidad de los Andes

November 24, 2016

A monograph submitted for the degree of Physicist

Supervisor:

Manu Forero-Shelton

Co-Supervisor:

Andrés González-Mancera

Acknowledgments

I would like to thank Manu and Andres for giving me their time and having patience throughout all the development of the work, especially during the time in which the development and advances where extremely slow. Also I want to thank my parents for not going mad with constant complaining about the slow development of this work and their constant and unrelenting support through my life.

And finally a special I want to mention some the many friends and colleges whose advices and word of encouragement made this work possible: Juan Felipe Mendez Aka “El Gallino”, Valentina Quiroga, Nicolas “Ill Doggo” Romero, Sergio Lobo, Mateo Restrepo, David Jaramillo, Sebastian Franco, Nicolas Morales Aka “El Mow”, Jesus “Fifu” Cifuentes, Jesus Prada, Andres Vargas, Mariana Londoño, Rafael Mariño, Roberto Moran (for allowing me to live in the IP 002), Santiago Monroy, Esteban Rivera, Maria Camila Garcia, and Lucas Varela.

Abstract

During *E.* coli infection of the urinary tract, bacteria are able to withstand significant forces from fluid flow. Bacteria are anchored to the surface via Type 1 fimbriae which have adhesive molecules called FimH at its distal end. *In vivo* studies of fimbriae attachment are difficult to perform due to the small size of these structures. In order to gain insight on how FimH catch bonds and fimbriae dynamics are coupled in the context of adhesion and fluid flow, we developed a computer simulation based on the Lattice-Boltzmann method (LBM) coupled to a dynamic simulation of the fimbriae. LBM offers advantages over traditional numerical solution of the Navier-Stokes equations such as being highly parallelizable and that complex boundary conditions can be easily programmed. A three dimensional realistic model of bacteria with adhesive structures was developed and the interaction between flow, bacteria and fimbriae was analyzed.

Resumen

Durante la infección del tracto urinario los *E.*coli son capaces de resistir las fuerzas del flujo. Las bacterias se anclan a la superficie por medio de fimbrias con moléculas adhesivas en sus extremos distales llamadas FimH. Los estudios in vivo de la adhesión de fimbrias son difíciles de realizar debido a que estas estructuras son muy pequeñas. Entonces para obtener información acerca de cómo los Catch Bonds de FimH y la dinámica de las fimbrias se acoplan en el contexto de adhesión y en un flujo de un fluido, se ha desarrollado una simulación computacional basada en el *Método de Lattice Boltzman* (MLB) acoplada a una simulación dinámica de las fimbrias. MLB es más ventajoso sobre otro métodos debido a que es altamente paralelizadle y permite implementar condiciones de frontera más complejas con mayor simplicidad. Un modelo realista, tridimensional de la bacteria con sus estructuras adhesivas fue implementado y la interacción entre el flujo, la bacteria y la fimbria fue analizada.

Table of Contents

Table of Figures

Introduction

The purpose of this work is to simulate the adhesion process of *E.* coli under fluid flow. To do so, it is necessary to successfully simulate the force and torque done by the fluid over the bacterium, the force and torque that pili make over the bacterium (which is a non-linear response), and the adhesion between pili and walls. The final aim of this work is observe the collective behavior of the system in different scales: Micro (fluid), Meso (pili), and Nano (adhesive molecules), and also the cooperative behavior of the pili. In particular, one of the things that we are interest in seeing is the collective behavior of the system when the bacteria moves against the current, as observed by [1]. The motivation for studying this phenomenon is to model infections that occur within the urinary tract, so understanding this scenario in detail is valuable for developing treatments for these kinds of infections; especially considering that they are becoming harder to treat as bacteria develop resistance to antibiotics.

Past works have studied how uropathogenic *E.* coli are capable of withstanding fluid flows by using imaging techniques, force spectroscopy, and flow-chamber experiments. But the use of simulations is necessary because it is not easy to see *in vivo* this system as it relates various mechanical properties at various scales. One of those works is [2]; here, a simplified situation was simulated where the pili were considered as only Hookean springs and while a stochastic simulation was used for the Catch Bond. The focus was to study how the bacteria can roll in the direction of a flow but after a critical velocity the bacteria seem to anchor on the surface. Additionally, it was noticed that this behavior is tolerant to the changes in the parameters.

Considering that the central aim of this work is the study of cooperation between the pili and the mechanism at various scales, it is valuable to remark that computational approaches have been successful in studying this kind of properties. In particular, [3] shows through a simplified scenario

to two dimensions that the pili works as a damper that allows the Catch Bonds to enters their more resistant state, a clear example of cooperation between mechanism at different scales. Additionally in [2], the method of Monte Carlo–Metropolis was used to simulate the stochastic behavior of adhesion, and it was possible to observe that the life-time of a bond depends on the amount of cooperation between the pili. This cooperation in turn depends of the mechanical properties (like its helical structure and its ability to unbind), which itself depends on the length of the subunits and the energy of the bonds. In particular, it was observed that by decreasing the characteristic length of the bond by half the lifetime decreased by three orders of magnitude.

This work intends to be different from previous work in the following aspects; first of all, a very important feature of this work is the use of *Lattice-Boltzmann* as a mean to simulate the behavior of the fluid which acts upon bacteria. Various previous work limit themselves to use numerical simulation in lower dimensionality [3]. The use of *Lattice-Boltzmann* allows the use of higher dimensionality and a more accurate geometry. Second, previous works have limited themselves in the use of stochastic simulation for the pili and the catch-bond, by considering only one of them; here both will be simulated that way. One of the refinements considered here is that pili have rigid properties, something already done in [2] but only without considering fluctuations in the structure of the pili.

The structure of this work will be the following, in the initial chapter all the individual components of the code will be explained and their validation will be shown. After this, the scheme of integration use will be presented and the basic simulation using the integrated code will be presented as well as their results. Additional, considerations for the rigidity of pili will be made.

Individual Components and their validation

Adhesion of Catch Bonds

Certain receptor-ligand bonds have shown an increase in their average life-time when a tensile mechanical force is applied over them, these bonds are referred to as Catch Bonds. A kind of Catch Bond (FimH) is present at the distal ends of type 1 pili of *E.* coli, so its simulation is necessary to describe the behavior of the adhesion. The FimH adhesive showcases affinity towards mannosylated proteins, which are present in uroepithelial cells.

The behavior of the Catch Bond is the following; the possible configurations of any molecule (including FimH) can be understood as an energy landscape where all possible configurations of a molecule are described by the degrees of freedom of the molecule itself. These degrees of freedom have a corresponding energy, so if particles have N degrees of freedom; it has a energy landscape with N+1 dimensions where the extra dimension is the energy associated with each configuration. In this space, local minimums are potential wells where the system is stable, and it is called structural state. If a system is inside one of those wells there is a certain rate for the system to escape them, which is explain by the Bell model [4].

$$k = A \cdot e^{\frac{-\Delta E}{k_b \cdot T}}$$

Equation 1

The parameters are the following: ΔE is the energy barrier that is necessary to overcome to achieve a state transition, $k_b \cdot T$ is the thermal energy, and A is the Arrhenius constant.

The idea behind this rate is the following; the structural states are the means of all the conformational states of a molecule (which depends on the velocities and positions of the individual particles that make them up). It is possible that the conformational states segregate around various

means, and because of that there can be various structural states for the molecule. The probability of existing at one of the various structural states is given by the Boltzmann's law, which states that the equilibrium between two structural states is given in function of the free energy of the conformational state, Equation 2 . This equation basically states that the equilibrium is given by the ratio of the two transition rates (as given by Equation 1).

$$k_{eq} = \frac{k_a}{k_b} = e^{\left(-(G_a - G_b)/k_b \cdot T\right)}$$

Equation 2

To achieve a transition between two structural states (G_1 and G_2), a transition state must be reached which is expressed as a potential barrier (G_A), Equation 3.

$$k_{eq} = \frac{k_1}{k_a} = e^{\left(-(G_a - G_1)/k_b \cdot T\right)} = e^{\left(-(\Delta G_{a1})/k_b \cdot T\right)}$$

Equation 3

The idea is that to change from one state to other a molecule must first gain certain activation energy, identified by height of the potential barrier, G_A of the transition state.

$$k_1 = A \cdot k_a \cdot e^{\left(-(\Delta G_{a1})/k_b \cdot T\right)}$$

Equation 4

The factor $A \cdot k_a$ is called the frequency factor or the Arrhenius factor. This factor can be seen as the frequency at which a molecule can arrive over the transition into the other conformational state only through diffusion. This can be affected by force through Equation 5:

$$k(f) = A \cdot e^{\frac{-\Delta E + f \cdot \Delta x}{k_b \cdot T}} = k^o \cdot e^{\frac{f \cdot \Delta x}{k_b \cdot T}}$$

Equation 5

The idea is that by deforming the proteins in a certain direction there is a tilting in the energy landscape and by that changing the energy barrier between the states and by that the rate of transition.

In the case of the Catch Bond, there exist two structural states (where one is deeper than the other). The force applied to the systems lowers the barrier between the wells enough, so the transition rate between them becomes higher allowing the conformation to change to the more stable state. In terms of the master equation, the system is described by Equation 6 and Equation 7.

$$\dot{p_1} = -k_{10}(f) - k_{12}(f)$$

Equation 6

$$\dot{p_2} = -k_{20}(f) - k_{21}(f)$$

Equation 7

In the notation used, state zero is used to define unattached state of Catch Bond, state one is the state with a lower life-time, and the state two is the state with the high life-span.

As the evolution of the system depends on the transition rates, a good way to simulate is through the application of the Gillespie Algorithm. This algorithm provides a solution to the master equation, which describes the evolution of the system. This is the sequence of steps of the algorithm:

- The rates of transition are normalized so their sum is equal to one and different sections of the interval [0, 1] are assigned to each rate.
- A uniform random number between one and zero is generated and depending where it lands in the interval a different action takes place.
- The moment in which the selected event takes place is decided through an exponential distribution, whose mean is equal to the sum of all rates of transition.
- For this particular case, the system begins in the state one and then changes into the state two (or the inverse), so the rates of $k_{10}(f)$ and $k_{12}(f)$ are exchanged for $k_{20}(f)$ and $k_{21}(f)$.

For the validation the following was done, a sample of 5000000 simulations of FimH was exposed to the same force. Over time all individual simulation end as the FimH escapes the well so a plot of the fraction that remain it each instant of time is done. From it can be seen that for higher forces the survival fraction becomes higher, which is consistent with the expected behavior of the Catch Bond. Additionally, the results were compared to experimental observations of [5]. The comparison (shown in the second plot of Figure 1) verifies that the situation correctly follow the experimental data.

Another test was made where samples of 80000 simulations of FimH were exposed to a constant force in the range between 0 and 100 pN units all Simulations ended. For each sample, the average time it took all the individual simulation to end was register. This trajectory was plotted together with identical simulation but considering only state 1 and state 2.

The result obtained in Figure 2 validates the effectiveness of this simulation as it shows the expected behavior as the mean-life time increases as the force also increased until an inflection point is reached and the life time begins to sharply decrease. Also, it can be seen that in the regime of small force the Catch Bond system exists near state one, but as force increases the population begins to migrate to the other state and eventually it all changes to the second state as the Catch Bond population and the population in state 2 begin to decay at the same rate. The parameters used for the simulation are presented in the

Table 1.

Parameters	Value from [5]
$k_b \cdot T$	$4.1pN \cdot nm$
k_{10}	$5.77hz$
k_{20}	$0.007hz$
k_{21}	$0.105hz$
k_{12}	$0.21hz$
x_{10}	$0.19nm$
x_{20}	$0.176nm$
x_{21}	$-0.42nm$
x_{12}	$0.858nm$

Table 1

Figure 1. The simulation of the Catch Bond follows the behavior shown in experiments.

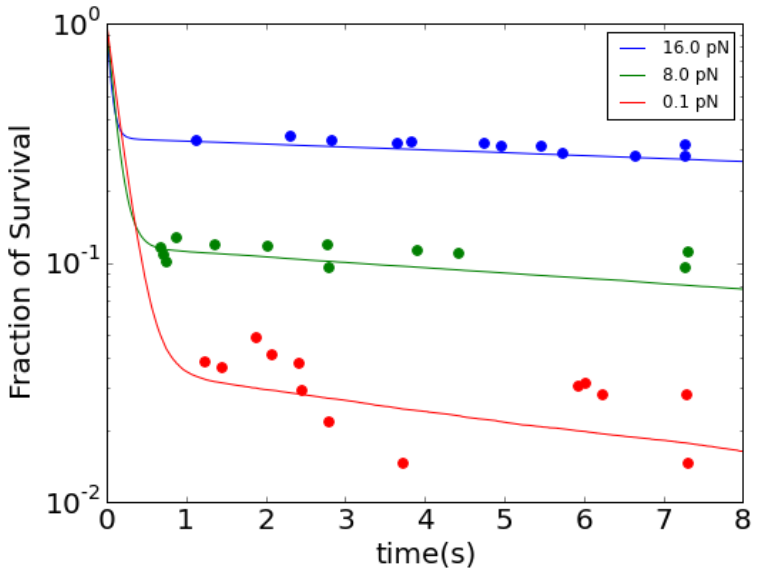

The trajectories given by the Gillespie algorithm (lines) follow the data set from reference (circles) [5] for the fraction of FimH molecules that survive for a given time (for three given forces). All the parameters used for the trajectories are taken form experimental data.

Figure 2 Simulation of the Decay of the FimH for various forces.

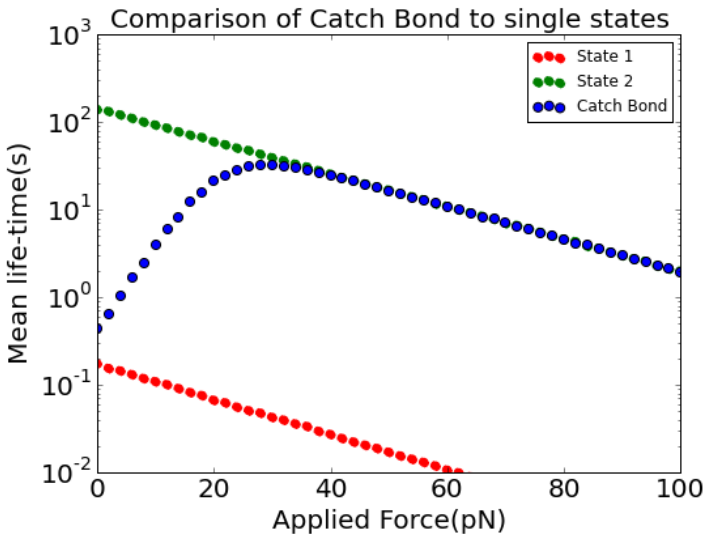

The simulation of the mean life time is correct as it shows the expected behavior (given by [5]), an initial growth as force increases, and then a strong decay as the force becomes too big. Additionally as force increases the Mean time of the Catch Bond becomes the same as the one of the strong state.

Pili

Type 1 Pili are organelles anchored to the outer membrane of Uropathogenic *E.* Coli. Their function is to facilitate the adherence to host cells which is essential in the initial steps of colonization. This kind of pili is mostly associated with bladder and lower urinary tract infections, and they are composed of FimA monomers which are arranged in a tight right-handed helical rod. In the distal end of it there are subunits of FimH and, FimG, in particular FimG is the responsible of the Catch Bond, [6].

It has been observed that under stress, type 1 pilus begins to unfold. This unfolding basically consists in that the quaternary structure made up of three units which creates a loop of the helical structure breaks (layer-to-layer bonds), leaving the monomers attach in chain-like structure

(head-to-tail bond). The section that is in the layer-to-layer bonds (all the entities related to this section use the sub index A) can be described as a Hookean spring (Equation 8) and head-to-tail (all the entities related to this section use the sub index B) section follows a model known as Worm like Chain (Equation 9) [2]. The parameters used in Equation 8 are the following: k_a is the elastic constant of the coiled unit, N_A is the amount of subunits in the coiled conformation, x_A is the total deformation of the coiled section, and L_A is the natural length of a coiled unit. The parameters used in Equation 9 are the following: $k_b \cdot T$ is the thermal energy, l_p the persistence length, x_B the length of the elongation in the uncoiled section, N_B is the number of sub-units in the uncoiled state, and L_B in the natural length of the uncoil sub-unit.

To calculate the force done by the deformation of the pili, the following is done; force is uniform in the springs that are connected in series, so the two expressions that describe the extension-force relations can be made equal (Equation 10).

$$F(x_A) = k_a \cdot \left(\frac{x_A}{N_A} - L_A\right)$$

Equation 8

$$F(x_B) = \frac{k_b \cdot T}{l_p} \cdot \left(\frac{1}{4} \cdot \left(1 - \frac{x_B}{N_B.L_B}\right)^{-2} - \frac{1}{4} + \frac{x_B}{N_B.L_B}\right)$$

Equation 9

$$k_a \cdot \left(\frac{x_A}{N_A} - L_A\right) = \frac{k_b \cdot T}{l_p} \cdot \left(\frac{1}{4} \cdot \left(1 - \frac{x_B}{N_B.L_B}\right)^{-2} - \frac{1}{4} + \frac{x_B}{N_B.L_B}\right)$$

Equation 10

In the system, the length of the Hookean section and the worm like chain section always adds up the total length, so this allows the elimination of x_A (Equation 11).

$$k_a \cdot \left(\frac{x_{tot} - x_B}{N_A} - L_A\right) = \frac{k_b \cdot T}{l_p} \cdot \left(\frac{1}{4} \cdot \left(1 - \frac{x_B}{N_B.L_B}\right)^{-2} - \frac{1}{4} + \frac{x_B}{N_B.L_B}\right)$$

Equation 11

This equation gives a cubic polynomial (Equation 12) whose real root is the length of the WLC. Then the solution can be find through the

$$4 \cdot (N_a \cdot b + c \cdot k_a) \cdot x_B^3 + c \cdot (-4 \cdot x_{tot} \cdot ka - 9 \cdot Na \cdot b + 4 \cdot a \cdot ka - 8 \cdot c \cdot ka) \cdot x_B^2 \pm 2.0 \cdot c^2$$
$$\cdot (-4 \cdot L \cdot ka - 3 \cdot Na \cdot b + 4 \cdot a \cdot ka - 2 \cdot c \cdot ka) \cdot x_B + 4 \cdot c^3 \cdot ka \cdot (-L + a)$$

$$a = La \cdot Na$$
$$b = k_b \cdot T / l_p$$
$$c = N_B.L_B$$

Equation 12

Because the force is equal in all sections of the spring, so by finding the length of the WLC section the force in that section is found, and which is the same as the force felt throughout all the pilus. For the pilus there are rates two transition rates, the opening rate for last close monomer and closing rate of the last closed monomer. Additionally, forces done upon the pilus alter the energy landscape in the same way they did in the case of the Catch-Bond (Equation 1).

For a dynamic evolution of the state of the monomers the Monte Carlo-Metropolis method is used, as proposed by [7]. For each time step, the rate of opening and closing are given by Equation 1. These rates are individually compared to a uniform random number contained in the interval [0, 1]. If the number is smaller than one rate then the transition is approved thus a change takes place, but if it is not higher nothing happens.

The results obtained are in Figure 3, which show the force-elongation trajectory for three different velocities. Here three stages can be appreciated; in the first one there is an almost linear increase of force with distance, as the Hookean has the dominating behavior. In the second stage, the force remains constant with the elongation; this is because force becomes big enough to make the transition from state A to B extremely likely so here the polymer begins to unwind sequentially. In the final stage, there is a nonlinear increment of force with extension; the reason is that all sub-units are now in the state B so the chain behaves like a WLC (Figure 3). The parameters selected for the simulation are in

Table 2.

Some additional remarks are that the number of subunits determines the amount of fluctuation in the flat section of the force elongation trajectory. The reason is that the deformation is equally shared among all the subunits that make up the coiled section and if the number of overall units is smaller than the deformation of individual monomers will be higher and this leads to bigger fluctuations in the flat section. The value of k shown is given for a coiled type 1, but the elastic constant of individual section is needed, so the following analysis is done. The force is the same throughout the spring, and then the force is the same for individual segments and for the whole pilus. Assuming that the deformations are equal distributed then individual monomers have a deformation which is a thousand part of the total, then to have a force equal to the whole pili the elastic constant needs to be about a thousand times bigger for the individual monomers.

In the Figure 4, the experimental measurements of the force found in the flat section are compared with the force obtained through the simulation. This comparison shows that the simulation replicates accurately the experimental observation by [6], including the fact that for small velocities the force in the flat section are almost constant and for higher velocities the change becomes far larger. An interesting thing to note is that the uncoiling behavior begins when the

probabilities to uncoiling and coiling are equal, which occur at values of about 30 pN [6], and in Figure 4 the uncoiling begins at 30 pN.

Parameter	Value
$k_b \cdot T$	$4.1pN \cdot nm$
k	$2.06\,\frac{pN}{nm}$ [4]
N_A	995
N_B	5
L_A	$0.7\ nm$ [1]
L_B	$5.7\ nm$ [1]
l_p	$1.2\ nm$ [8]
k_{AB}^0	$0.016hz$ [6]
k_{BA}^0	$1.875 \cdot 10^{14} hz$ [6]
x_{AB}	$0.59\ nm$ [6]
x_{BA}	$-4.41\ nm$ [6]

Table 2

Figure 3. Simulation of the response to elongation of the pilus for three different velocities.

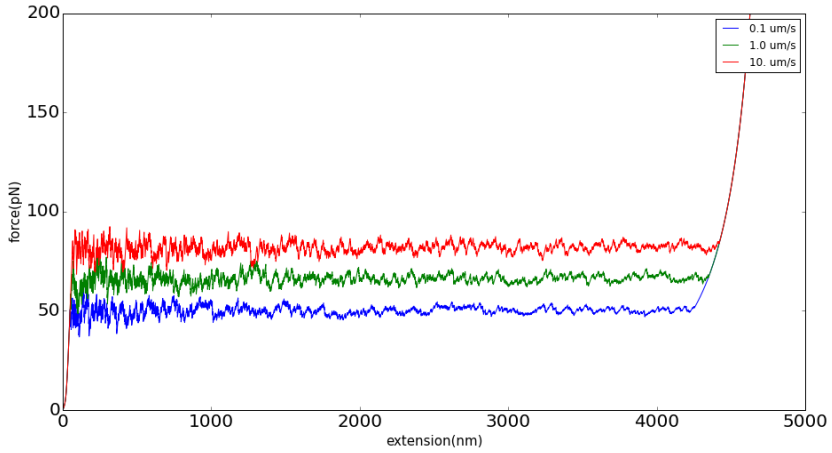

The simulation replicates the behavior expected from experimental results. There are three regimes, one of linear behavior, one where the force remains constant to changes in elongation, and a non-linear domain. Additionally the region of constant force is dependent of the elongation velocity.

Figure 4. Comparison of the simulation of the pilus to experimental data.

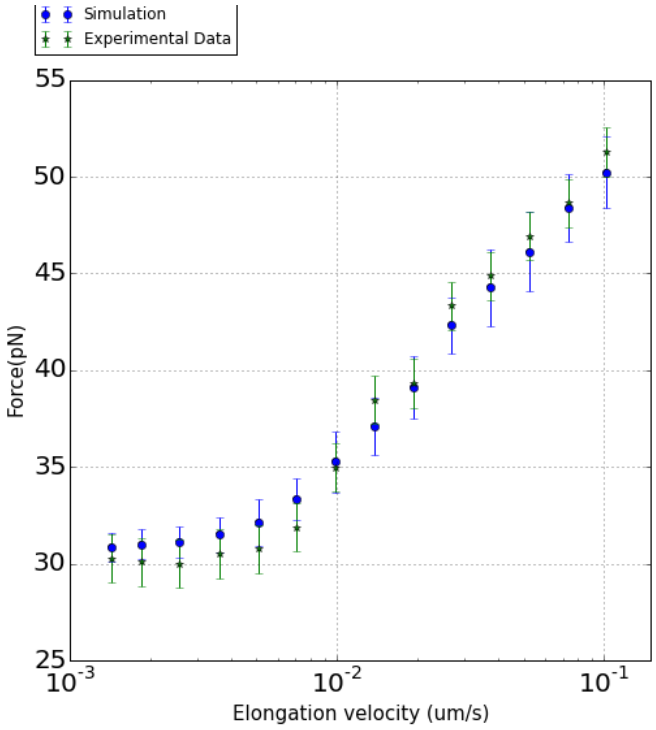

The simulation reproduces the expected values in the constant force regime (given by [6]) of the elongation of the pilus. The Simulation of the pilus is applied for various extension velocities and an average is obtain form the plane section.

Fluid

The fluid simulation requires a velocity profile which grows linearly in the direction of the coordinate z, this kind of profile is known as Couette flow (see Figure 5). This profile is used because in the urinary tract there is a parabolic profile, but it can be approximated to linear one if the distances which are being observed are very small. To create this profile is necessary a boundary condition with zero velocity and other with a non-zero velocity.

The computational method used to perform the simulation is *Lattice-Boltzmann* (all routines necessary to implement LBM were provided by the Palabos Library). Its basic idea consists that if one solves the Boltzmann discreetly together with a collision model, an approximate solution to the Navier-Stokes equation is obtained. The method is done in the following way: the space is turned into a discrete grid. In each instant of time, fictitious particles are going to move form a node of the

grid into another, and in the case that two or more particles arrive to the same node a model collision is applied which changes the trajectory of the particles involved in the collision. The general idea of this method is that by average of this microscopic behavior the macroscopic behavior emerges.

Figure 5. Boundary Conditions for the Domain.

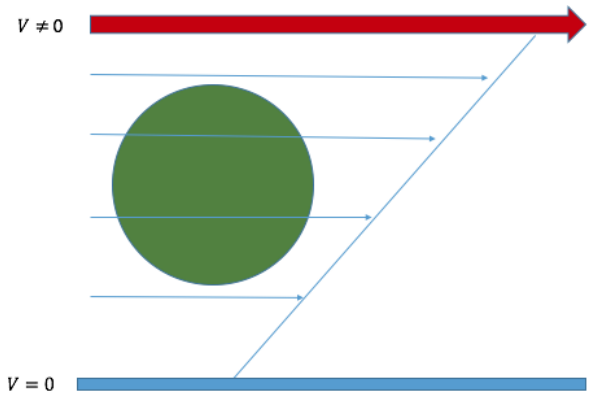

The Domain has two boundary conditions. A constant non zero force wall in the upper one and zero force in the lower boundary.

Explicitly, each node in position $\vec{x}$, in time t, has a density $f_i(\vec{x}, t)$. The sub-indexes denote the direction in which the particles propagate, for example for a certain node of position $\vec{x}$ the density $f_1(\vec{x}, t)$ gives the number of particles that move upward, the density $f_2(\vec{x}, t)$ gives the particles which move downward, and for each direction there is a density, in this case there are 19 each one each direction of propagation. Additionally, it is also; consider that the speed of propagation is just enough to arrive to nearest neighbor in a unit of time. Considering this, the time evolution of the system is the following: for in each instant to a node a number of particles arrive from the nearest neighbors, in the case of not considering some kind of collision then outgoing density would be the same as the incoming density (the same number of particles would be leaving to go upwards as the particle arriving from downwards).

If one considers collisions within the nodes, then the density will fluctuate and this leads to a change in the direction of propagation. This evolution is described by the following equation: where $f_i^0(\vec{x},t)$ is the density at equilibriumτ is the relaxation time, $f_i\left(\vec{x}+\overrightarrow{\delta_i},t+1\right)$ is the density in the neighbors' node in the next instant of time:

$$f_i\left(\vec{x}+\overrightarrow{\delta_i},t+1\right)=f_i(\vec{x},t)-\frac{1}{\tau}\left(f_i(\vec{x},t)-f_i^0(\vec{x},t)\right)$$

Equation 13

The terms that described the phenomenon of collision is: $\frac{1}{\tau}\left(f_i(\vec{x},t)-f_i^0(\vec{x},t)\right)$. It dependes of how close is the current density to the equilibrium one, which means that when the equilibrium is finally reached the collision effect vanishes. Also the collisions of the fictitious particles give the force generated by the flow over the bacterium. The parameter τ is called the relaxation time and it is responsible for the stability of the simulation, especially if it becomes smaller than 0.5 the simulation collapses. The relaxation time is given Equation 14.

$$\tau=C^2\cdot\mu_{lattice}+0.5$$

Equation 14

This quantity creates a relation between the density of the fluid in the lattice, the time step and the separation of the vertex in the lattice, as the three are requires obtaining the dynamic viscosity within the lattice. Due to the need of a time step small enough to describe accurately the evolution of the system but big enough to make the simulation something workable, there was the need to change the other values so relaxation time of about 1.833 was obtained.

The domain was constructed in the following way, on the upper and lower walls velocity boundary condition were imposed with the lower wall having a velocity of 0 and the upper of 8

mm/s, which correspond to shear of 2700 $pN/\mu m$ as given by [9]´. The lateral walls have free slip condition which means that they don't exchange momentum by contact. Finally the walls the walls perpendicular to the direction of the flow have continuity conditions. The domain considers a basic unit cell with 19 nodes (Figure 6).

Figure 6. Structure of the lattice.

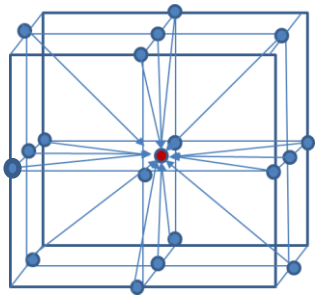

The characteristic cell of the domain is made up of 19 points. 18 from which molecules are released and one central which receives them as they propagate.

Two different comparisons were done to verify the results given by the simulation, on the first one a steady sphere was released in the flow and the time evolution of the sphere's linear and angular velocity was compared to what is expected from the calculations of [10], which states that the spheres eventually reaches a steady state where both the angular and linear velocity become constant. The second test consists of comparing the normalized torque and force given [10] to the simulation. The results Figure 7 show that indeed the sphere reaches this steady state and the values for the velocity are very close to the ones predicted, the divergences are at most of around two percent. Figure 8 show the comparison between the values of normalized torque and force given by the theory and obtained through numerical simulation, with relation to the ratio between the distance between the wall with zero velocity and the center of the sphere (h) and the radio of the sphere (a). The simulation parameters are in

Table 3. The parameters were selected with the intention replicating the characteristic of urine, and because urine is mainly water μ and ρ are thee same as the ones of water.

Parameters	Value	New units
V_o	$8\frac{mm}{s}$ [9]	0.0106
$m_{E.Coli}$	$1pg$	1
$R_{E.Coli}$	0.5 μm [1]	0.25
μ	$1.0 \cdot 10^{-3}\frac{N \cdot s}{m^2}$	0.002
ρ	$1.0 \cdot 10^{3}\frac{kg}{m^3}$	$8 \cdot 10^{6}$
Lattice units per real unit		
dt	10^{6}	
dx	$10^{3}/_{75}$	
$\rho_{lattice}$	$1.0 \cdot 10^{5}$	

Table 3

Figure 7. Simulation reaches linear and angular equilibrium velocities

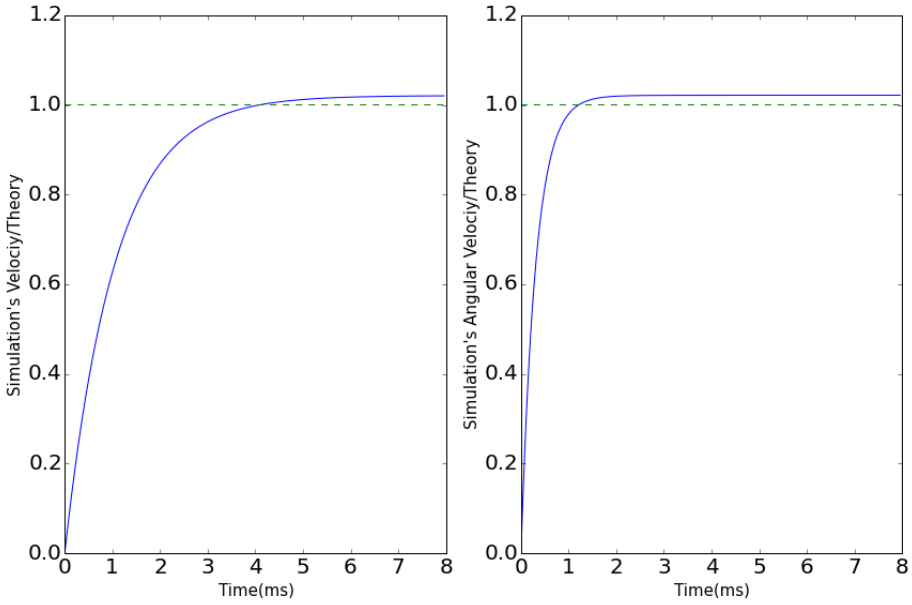

The velocities given by the simulation are normalized with the value given by [10] The values approach their expected values. The difference could be attributed to the approximations made in the analytic solution.

Figure 8. Comparison of the force and torque felt by the sphere as it approaches the zero velocity surface.

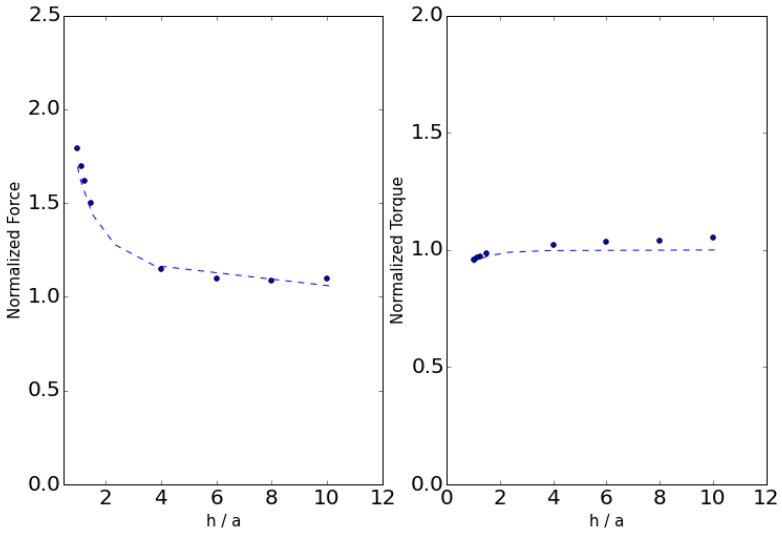

The values of line represent the values expected by the theory of [10] and the dots the values obtained by the simulation. The axes of the plot are the normalized force and torque against the ratio between the radius of the sphere and the distance between the center of it and the plane below.

Integration of the different components

Framework of the simulation

The core idea of the simulation to couple the codes previously shown in the following way: for each new time step there is a change on the position of the sphere, as well as a rotation, due to the action of the fluid. These displacements of the bacterium change the position of the pili over the surface below. In the case when the pilus is unanchored, it is assumed that the pilus is a straight ray perpendicular to the surface of the bacterium with a length equal to the number of subunits in the coiled states times their characteristic length, this is assumed because sub-units in the uncoiled state have no force acting over them and because of their condition of wormlike chain their effective length becomes zero. Those rays change position the same way every point the bacterium's surface does due to the torque and forces that act over it. If the distal end of the pilus approaches the plane, it may become attached due to the action of the catch-bond. When the attachment occurs the distal end becomes fixed in that position and every additional displacement will change of the pilus and in turn induce a force and a torque. This force, due to the third law of newton, will affect the rates of transition of catch-bond, allowing for a change in its conformational state.

Implementation of the Pili

For the execution of the pili, the only data required are the elongation of the pilus and the number of the monomers in each state in the pili. To obtain the total elongation for each individual pilus two positions are saved:

- The position of the distal extreme of the pilus.
- The position over the bacterium's surface where the pilus is located.

Using the position over the plane and over the sphere is possible to find the vector that connects both points, and then its norm is the total displacement. Using this value, the total the force can be found using the algorithm previously explained. Then the same vector of distance is normalized with the displacement and multiplied by the force found which gives the direction by which the force is acting. To find the torque, the cross product is done between the force vector and the vector that connects the point where the pilus is located over the sphere and the symmetry axis of the sphere parallel to that point.

It is assumed that the pili are always straight lines, in reality that may not happen as there are two sections in the pilus, one much thicker (coiled) than the other (uncoiled), so in the interphase a bending might occurs. It is supposed, that the torque and force will make these two sections align extremely fast. This assumption is useful as it simplifies the algorithm of the pilus because it removes the need of simulating the bending of the two sections. It also allows the use of the model of force of the pilus, because this model has the fundamental assumption that the force throughout the pilus is the same even if the sections follow different force elongation relations, and also that the force is parallel to the pilus. If the pilus bent that would not be the case, and all the work done to simulate the time evolution of the pilus would not be valid.

As the forces and torque move the bacterium, a pilus can approach the plane. There is a certain probability that the distal end of the pilus (where the FimH is present) will adhere to the mannosylated proteins and become fixed a position. This rate of initial binding, proposed by [2], is given by Equation 15, (where $x_{rms} = \sqrt{\frac{k_b \cdot T}{k}}$ describe the thermal fluctuations and $\boldsymbol{k_{0i}^0}$ is the rate of

adhesion for the when the pilus is in contact with the surface) and depends on the distance from the surface (d).

$$k_{0i} = k_{0i}^{0} \cdot erfc\left(\frac{d}{x_{rms} \cdot \sqrt{2}}\right)$$

Equation 15

To implement the binding rate a threshold distance of $5 \cdot x_{rms}$ is assumed, such that for distances below the binding rate is considered and beyond that point is ignored, this is done with the intention of ignoring this processes for distances for which the binding rate is insignificant. This is the same as done in [2].

Also an additional approximation is made, in reality there is a chance that the catch-bond enters directly to state 2, but it is neglected because it is insignificant in comparison to the rate of entering of directly to the state 1 (according to the values presented in [2] the value of k_{01} is higher than 3 Hz while the value of k_{02} is lower than 1e-6 Hz). Ignoring this rate has a great advantage of the simulation; it can be simulated in a very simple way by using Monte Carlo Metropolis, instead of using the Gillespie algorithm which would be necessary in the case of having the two rates and would create complication in relation to the random time at which the attachment occurs.

A difficulty encountered is that the time scales involved in the processes of the pili uncoiling are very different from the time scale used in the fluid simulation, which is necessary to ensure its stability. The solution encountered is the following, the transitions will be observed after a certain number of fluid iterations, this allows for a more significant elongation of the fimbriae and bigger transition probabilities. This has the added benefit of lowering computational cost as less random number will be needed. It is necessary to find the correct partition of time for the pili because if it is too small the simulation will not have resolution to see the sequential unbinding of

the chain and, if it is too big too many random will be used but without any significant improvement in the simulation, making the simulation costlier without improvements.

The idea is to observe how the mean and the std. deviation of the force in the plane section behaves for a given elongation speed by changing the *dt*. The results of these experiments are show in Figure 9. This experiment is done for extension velocities of 0.1 um/s, 1 um/s and 10 um/s. As it can be seen in the three following plots, for a *dt* small enough both the mean and the deviation present huge increases, and as *dt* begins to decrease there is a global minimum and finally both values become constant (with some small fluctuations). This is because for a *dt* big enough the transition probabilities become so big that in a single step all the monomers switch from the coiled state to the uncoiled state making that the only behaviors exhibited are the Hookean one and the WLC. In the global minimum, the *dt* is just big enough to resolve the uncoiling of the chain, but in a very poor way.

As it can be seen in Figure 10, there is a shift in the position of the minimum in response to a change in the elongation velocity (which is logic as a smaller *dt* would be required to resolve an event that has a higher speed). Using this result, then it can be concluded that the *dt* necessary for the simulation should be one around 10^{-4} s, as the velocities at which the bacteria is exposed are around the order of 10 um/s, and this value work equally well for lower velocities, so considering that the time interval of the fluid is of 10^{-6} then every hundred fluid iteration the pilus evolution would be executed.

Figure 9. Behavior of the mean and the std. deviation of the pilus simulation as the dt changes.

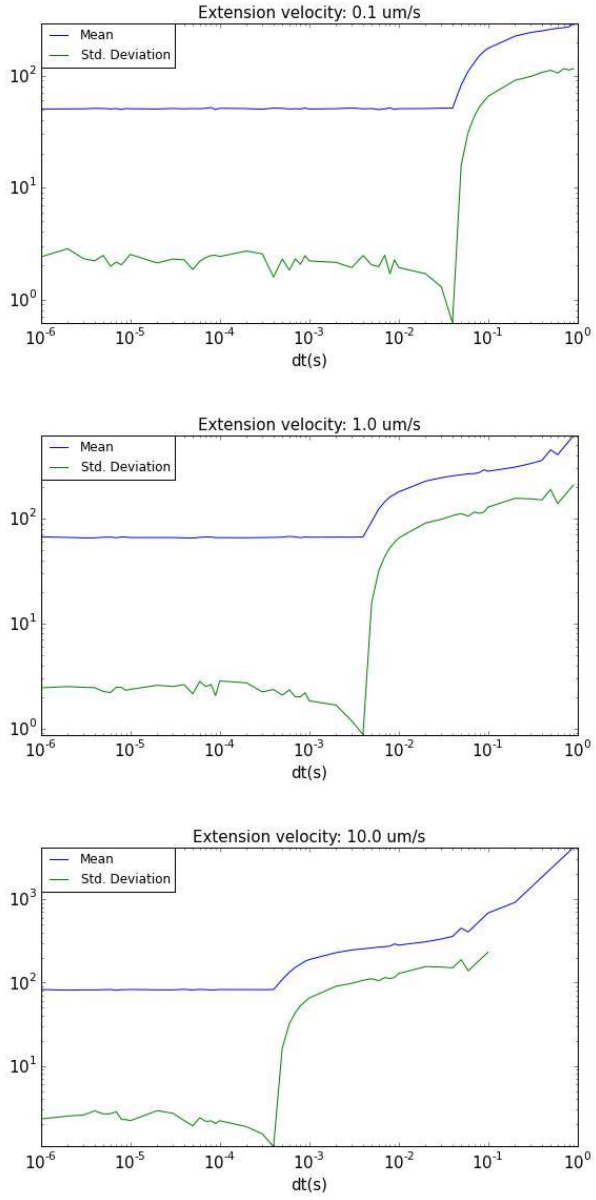

The plots show that for high values of dt, the simulation has a large deviation and an equally large mean. The reason behind this is that for those values the sequential uncoiling occurs too fast and the behavior is dominated by the non-linear increase in force. As the dt reduces there is a reduction only until the mean reaches a plateau and the std. deviation gets to a global minimum, the reason is that in this point the sequential uncoiling occurs proving a plateau of force, but the fluctuation are very small. Further reduction of the dt does not change the mean or the std. deviation.

-

Figure 10. Comparison of the std. deviation for different velocities.

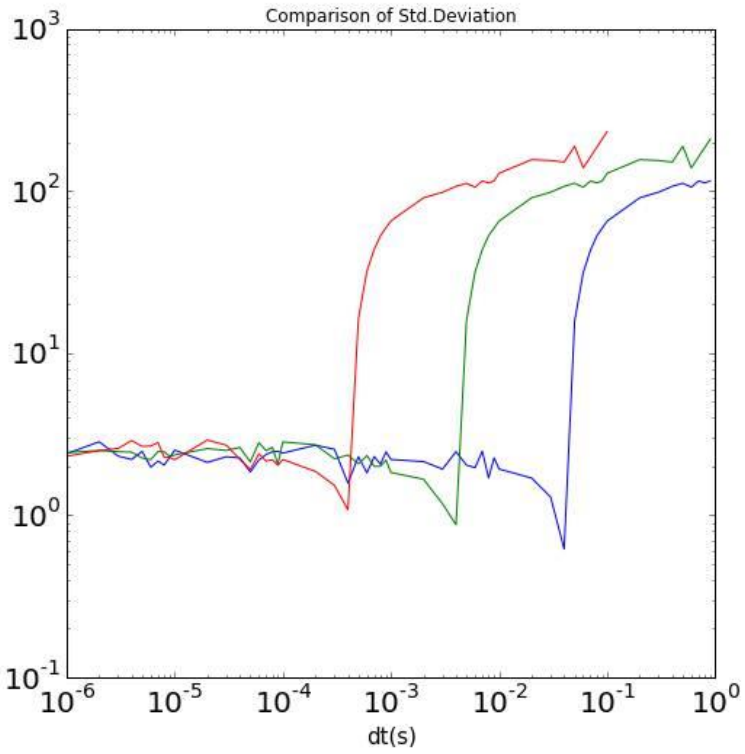

The minimum is when the uncoiling can be resolved, and it is dependent of the velocity at which the uncoiling takes place.

Implementation of the Catch Bond

For the implementation of Catch Bond there is a problem that comes directly from the use of the Gillespie algorithm, this algorithm gives the time in which a transition of state will take place, but only if the rates remain constant until during that period of time. This supposition does not hold in the system that is being studied because the rates may change in each time step because of the external forces of the fluid and the pili.

The solution proposed is that the transition will be observed in time lapses when the bacteria is stationary, understood as moments when the bacterium is under the influence of a constant force. This is done is done by comparing the force in one iterations to the one during the previous iteration. As long as the forces remain approximately constant the time for transition given by the Gillespie is respected. Also if a transition time takes place between iteration it will allowed because during the time between iterations the force is constant.

The approximation will ignore the possible effects that the different that the changing rate would have before the bacterium reaches the steady state. As it can be seen in Figure 11 , which shows the average time it takes for a transition to take place in both the state 1 and the state 2 (which is given by the inverse of the addition of the rates involved in each state), in comparison to the time step used in the simulation. The plot clearly shows that the difference between the time step and the average time for both state 1 and state 2 is enormous and the average times only approach the time step if the forces involved in the system are of an order of around 100 pN. The system reaches only force of the order of 10 pN, so transition that take place within single iteration are extremely unlikely (their mean time is of the order of a 1000 iterations). Considering this it can be assumed, that the dynamics states in the movement of the bacteria take place too fast to allow a change and only in steady state enough time can pass to make a transition likely.

Figure 11. Comparison at which a transition takes place for various force and the time step used

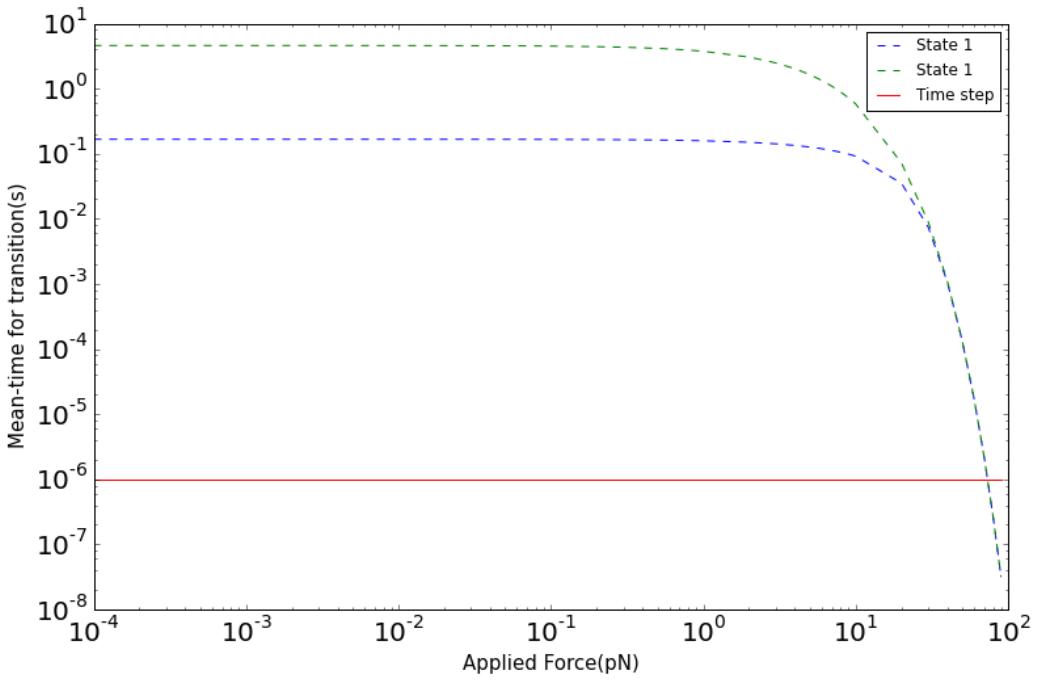

The difference between a time step at which an event takes place and the time step are very far away force low force domains and closer as the force increases.

Integration scheme

The integration scheme can be fully develop with the implementation of the pili and the catch-bond shown previously. The first step, the bacterium moves and rotates. After that, all the pili are observed, to find which ones can adhered to the surface below (depending on how close each one is to the plane and in which state their catch-bond is) by using the transition probability given by Equation 15. For each individual pilus that is attach to the surface the implementation for the pilus previously explained is used, but there an additional constrain and is that if the distance between the distance between the position over the sphere and the surface is lower than its minimum length, that is the length corresponding only to its coiled length, then no force is produced by the pilus.

The force of pili is used in the implementation of the catch-bond previously presented, to see if any evolution takes place. Also the force and torque of pili are added to the torque and forces done by the fluid to obtain the total force and torque. This total torque and force is used to change the both the angular and linear velocity of the bacterium, those velocities in turn are used to move the bacterium. This process is then repeated to allow the system to evolve. An extra condition is applied to the lower wall, to prevent the bacterium from escaping the domain; the velocity becomes zero in the component perpendicular to the wall if sphere directly collides to it.

One Pilus

The first simulation done which applies all the methodology previously explain is the simples scenario when the bacterium is anchored by only one pilus which is located in the lower pole of the sphere (see Figure 12). This initial model allows the study of two interesting parts of the system in question, first, how is the trajectory of the bacterium when a single pilus acts like an anchors and disturbs the motion of the bacterium; second, how is the response of the pilus to a sudden change in the shear of the flow.

Figure 12 Position of the pilus when the simulation starts.

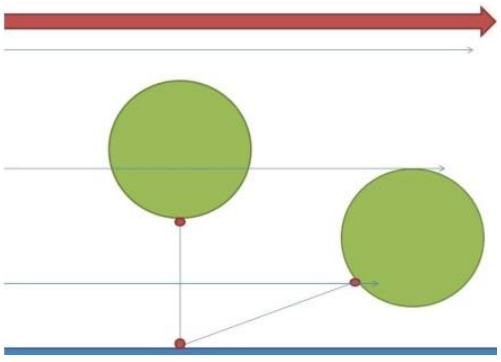

Bacterium´s trajectory

The following is done to observe how the bacterium's trajectory changes when it is pulled by a single anchored pilus: an identical domain is initialized with different velocities in the upper boundary. This velocity gives rise to a shear stress which is given by the following expression (where s is the rate at which the speed of the flow changes with height). μ is the kinematic viscosity of the fluid and u is the function which gives the velocity of the fluid in every point.

$$\tau(y) = \mu \cdot \frac{\partial u}{\partial z} \rightarrow \mu \cdot s$$

Equation 16

The following things can be noted from Figure 11, the first being that the trajectories are not circular as the case of a stiff rod will be. Second that as the shear increases the place at which the bacterium hits the ground increases. The reason behind these two observations is that pilus particular force elongation relation. As it can be seen in Figure 14 for lower shears, the distance from the rotation axis remain almost constant as the pilus stays in the Hookean regimen where it can respond to the changes in force as the bacterium descends. As the shear increases there are larger forces made upon the sphere which make the produce larger displacements that make the pilus enter the constant force regimen.

An important thing to note is that the constant force regimen at which the pilus arrives is big enough to allow an extremely fast transition of the catch-bond into the more resistant state. This can be seen as a way for the bacterium to assure the survival of an initial attachment under condition of extreme shear.

Figure 13. Trajectory of the bacterium under the influence of a single pilus and the fluid.

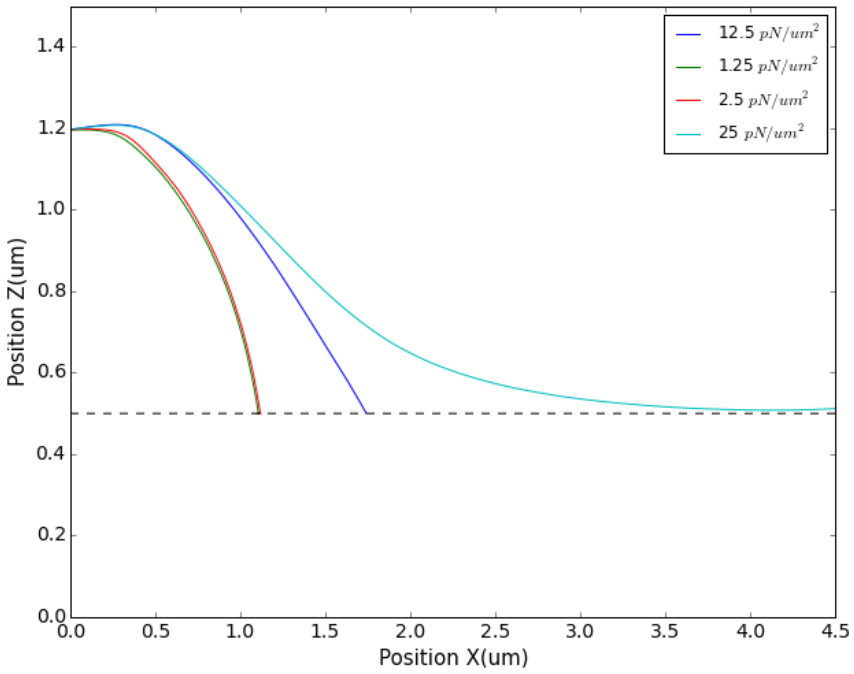

For low shear the trajectory is almost circular as there is no deformation and the pilus works basically as a rod. As the force increased there is a deformation in the pilus as it falls, this allows an increase in the distance at which the bacterium hits the ground. The dotted line indicates the radius of the bacterium.

Figure 14. Force in the Pilus during the fall.

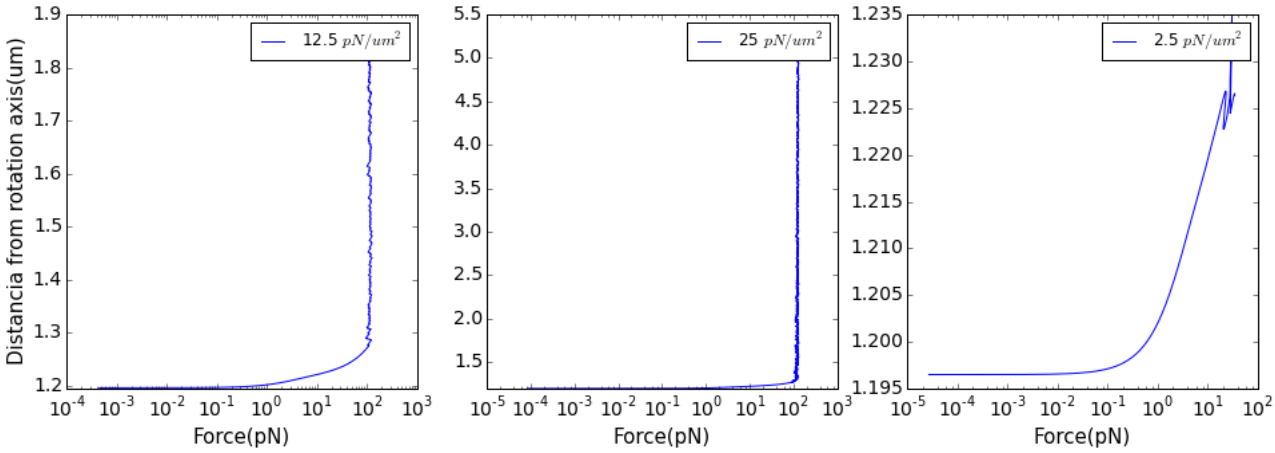

The force of the pilus is dependent of the shear of the fluid, at higher shear the force of the pilus will increase until it reaches the uncoiling point. It can be noted that the constant force that appears is enough to produce a fast change in the catch-bond, and allow it to enter the strong state.

Response to changes in shear

The bacterium is exposed to 0.1 s to a shear of 7.5 pN/ (um) ^{2} and then to a shear of 0.25 pN/ (um) ^{2} for the same period of time. The results are presented in Figure 15, as it can be seen during the high shear time there is an uncoiling, but as soon as there is a change in the shear the uncoiling suddenly stop and there is a recoiling which in turn pull the bacterium to its initial position. The mechanics present here are the follow, during the high shear time the forces are high enough to overcome the forces that pilus produces and have a net force that can alter the transition rate enough to make the uncoiling an extremely likely event. When the shear reduces, the force done the fluid reduces, so the net force reduces enough so the recoiling becomes the most likely event in the pilus.

Figure 15. The effects of a change of shear for the position and the uncoiling if the pilus.

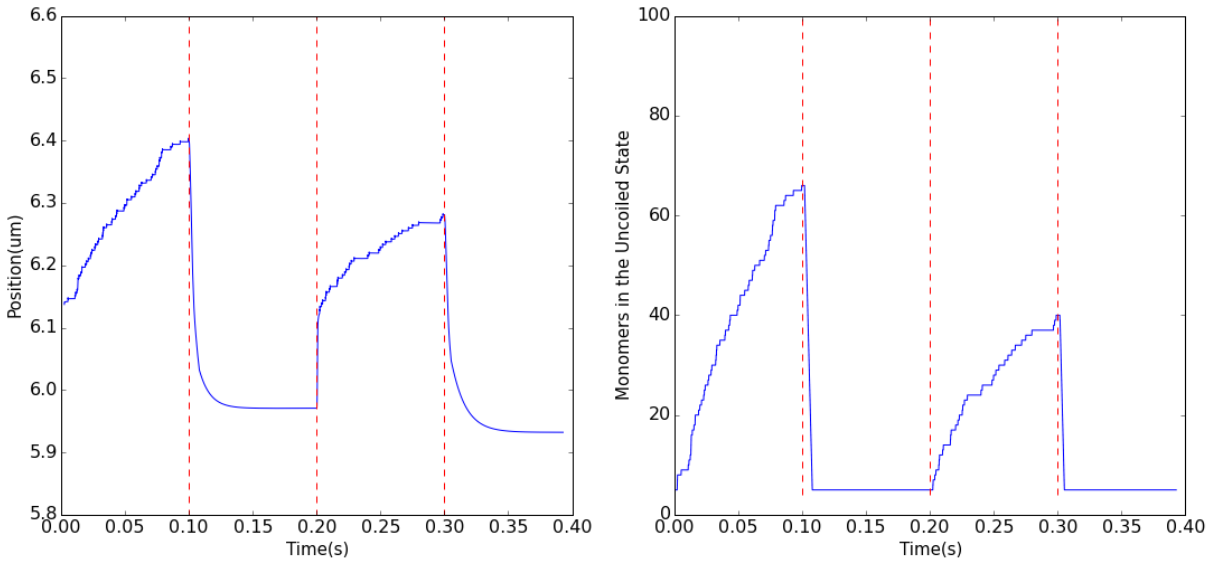

Here a periodic change of shear is made every 0.1 seconds (between 7.5 pN/ um^2 and 0.25 pN/ um^2). For the initial high shear the pilus uncoils. When the shear is decreased the pilus recoils and pulls the bacterium back again. When the high flow is increased the behavior repeats again.

Multiple Pili

For the application of the code using multiple pili, the pili are randomly distributed over the surface of a sphere with the intention of not including any bias about their position. This is done by generating 2 random uniform numbers, one in the interval between 0 and π, and other between 0 and 2π and used them as θ and φ in the spherical coordinates system.

The results are presented in Figure 16 (for the case of ten pili scatered over the bacteriums surface), and considering a change in velocity equal to the one used for the case of a single pilus, each red line demarks the point at which the velocity changes (the initial domain is the one with high shear). The behavior of retraccion can be apreciated in the results, during the periods of high shear there is a foward motion, but in the lower shear domain the retraction of the pili is able to generate upstream movement of the bacterium.

The decrease in the position in each repetition of increase and decrease of the shear can be attributed to the more of points of anchoring in each interation and the increase in force they make. As it can be seen Figure 17, the initial point of anchoring is the Pilus 3, which present an enourmous increase in force in response to the displacement done by the fluid, and as the bacterium moves 2 more additional anchoring points appears (Pilus 0 and 5), as soon as there is a change in the shear there is a pull backward. In the next iteration, another anchoring point appears and produces a additional force backwards, and for the thrid iteration there are 4 addionatal anchoring points making force.

Figure 16. Bacterium exposed to a period change in shear

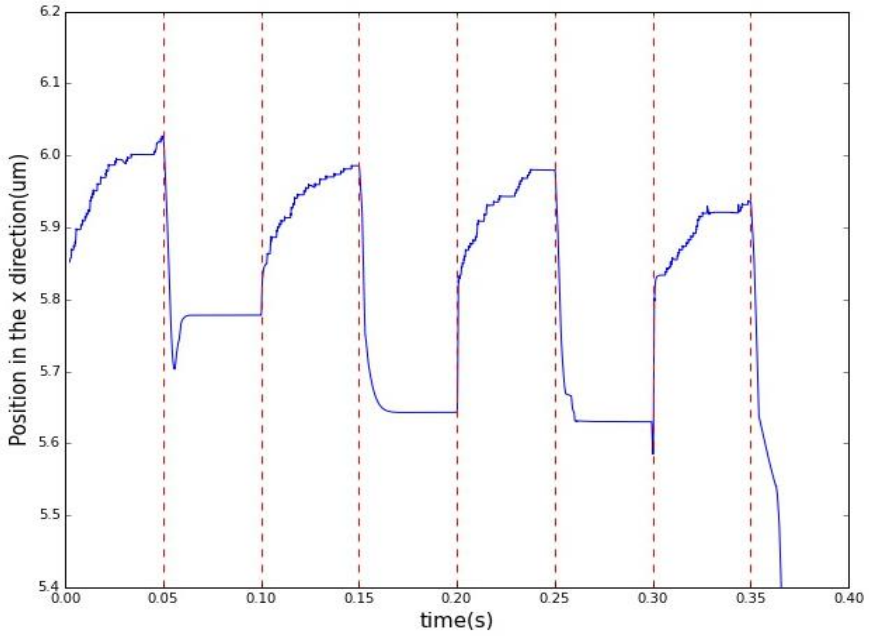

The shear is changed between a high regimen and a low regimen. It can be seen that during the low regimes the bacterium goes backwards due to the pili retraction. The red lines indicate change in shear regimen. There is a reduction of the net distance in every iteration. The changes in shear are periodic between 7.5 pN/ (um) ^{2} and 0.25 pN/ (um) $^{2.}$

Figure 17. Force for individual pilus

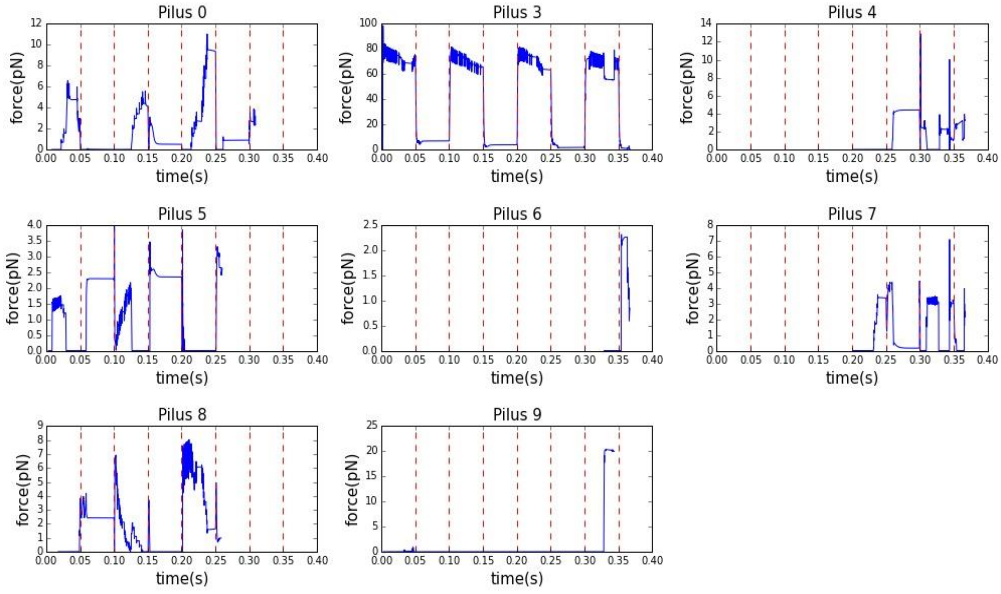

The response of individual pilus due to the change in shear. The leading pilus is the pilus 3 but the force begins to distribute between them as more begin to anchor (principopallu Pilus 5 and 8). The changes in shear are periodic between 7.5 pN/ (um) 2 and 0.25 pN/ (um) 2.

Mechanical properties of coiled pili

The addition of the condition of rigidity for the pilus requires the inclusion of two new properties, force due the bending of the pilus and force as a response to compression of it.

Bending

The force required for the bending of a rod to a certain curvature 1/R is proportional to the force applied times the distance at which the force is applied Equation 17. The EI is referred as the flexural rigidity, the quantity can be simplified by assuming that the material being bend is isotropic and homogenous, so the direction of the bend does not affect the curvature of the bending. Because the structure of the pili type 1 has a helical symmetry; it can be assumed that it is independent of the direction of the bending. This allows the flexural rigidity to be separated in two terms, the young modulus (*E*) which is a measure of the stiffness of a material and the second moment of inertia (*I*) that is determined by shape of the rod. These two values for the case of the pili type 1 are already measured and given by [2].

$$F \cdot x = EI \cdot \frac{1}{R}$$

Equation 17

A simple method to take into account this affect is through the use of the cantilever equation (Equation 18), as seen in [11]. The cantilever equation suggests the deformation for a rod that is clamped at one end, and has a transverse force applied to the free end of it (see Figure 18).

$$k = \frac{F}{y(L)} = \frac{3EI}{L^3} \rightarrow y(L) \cdot \frac{L^3}{3EI} = F$$

Equation 18

Figure 18. Scheme of cantilever force

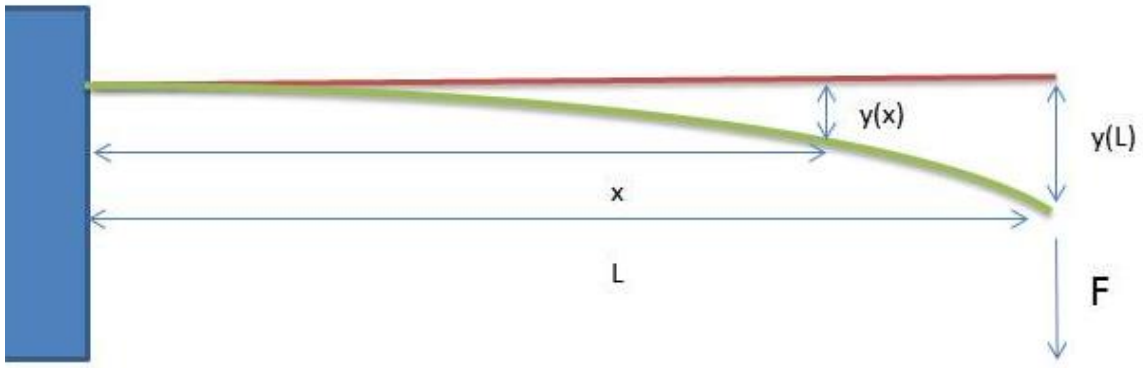

The cantilever produces a restorative force in response to a deflection form the equilibrium position, which is when the rod is completely perpendicular to the plane to which it is clamped.

The cantilever equation (Equation 18) is extremely useful and a more detail solution would be beyond the scope of this work. This method becomes even more useful if it is use in conjunction with the previous assumption that uncoiled and coiled sections are in parallel. Then by only using the unitary vector in the direction of pilus (the vector between the point of anchoring in the plain and the position over there sphere) and multiplying it by the distance of the coil section (which would be the number of coil sub-units times their characteristic length) the position of the distal end of the deformed section is known. Then is only necessary to obtain the position of the rest state (which is the normal vector to the sphere in the point in which the pilus is located over the sphere surface times the distance of the coil section) and subtract these two vectors. The norm of the resulting vector is total deformation which in turn gives the force due to bending. The use of this approximation has precedent in [2].

Buckling

The compression of a rod can result in the buckle of the beam into a sinusoidal shape. The buckle only begins after a critical force given by the Equation 1 is reached, [11].

$$F_c = \pi^2 \cdot \frac{EI}{L^2}$$

Equation 19

For the modeling of the compression the same assumption made by [2], is done here, the pilus is incompressible while the force made is below the value of the bucking force.

When the bacterium collides with one of its pilus, it applies a component of its momentum over the direction of the bacterium over them period of time corresponding to an iteration. As the pilus is incompressibility, it returns a force in the same direction but with negative magnitude. Considering the pilus moves, the force would not be necessary in the direction radial to the bacterium, so it could produce a torque.

To identify which pili are compressed by the bacterium is necessary to establish which ones are in the way of the movement, for this the following condition are establish:

- The dot product between the vector velocity and the vector parallel to the pilus must be bigger than zero.
- The z component of the vector parallel of the pilus is 0.
- The distance between the distal end and the point over the sphere must be the same as the number of coil units time their length.

The first condition is necessary to locate pili that are in a position which compression can occur; which is the half the sphere with radial vectors which have a component parallel to the direction of the motion. The second condition is necessary to assure that the pilus is indeed touching the surface of the plane below. The third condition is necessary as only the coiled section has the properties of rigidity.

Fully integrate simulation

The addition of the rigidity of the pilus allows fuller analysis of the elements at play during the phase of adhesion. A seen in the analysis of a single pilus, the first attachment (which is the first one that anchors the bacterium) quickly enters to the state 2 of the Catch Bond (see Pilus 3, Figure 19). This pilus alone withstands the initial pull of the fluid and this leads to a sequential uncoiling of it structure (see Pilus 3, Figure 20). The overall elongation during this instance is lower compared to the case where the pili lack rigidity, this is because additionally to the effect of additional anchoring points (as the case without rigidity), and pili in the way of the movement can damp the motion of the sphere. Also it can be noted that in the case without rigidity the position is not constant, but increases until the shear is lowered, in this case a stable position is reached, and the reason is that the pili at dampening the motion are not allowing the bacterium to move further.

As the flow changes shear, the force done over the sphere by the fluid reduces and the retractile force of the single pilus is able to pull the bacterium backwards (see first sector, Figure 22). During the low shear period, an additional pilus attaches to the surface (see Pilus 2, Figure 19). During the second period of high shear these two pili reduce the displacement done by the fluid and the Pilus enters into the second state of the Catch Bond. During the decrease in shear a third pilus enters the second state of the Catch Bond (see Pilus 8, Figure 19). With this third additional pilus, the overall force over each pilus is not high enough to produce further uncoiling.

Figure 19. Time Evolution of individual pili that enter the strong state of the catch-bond

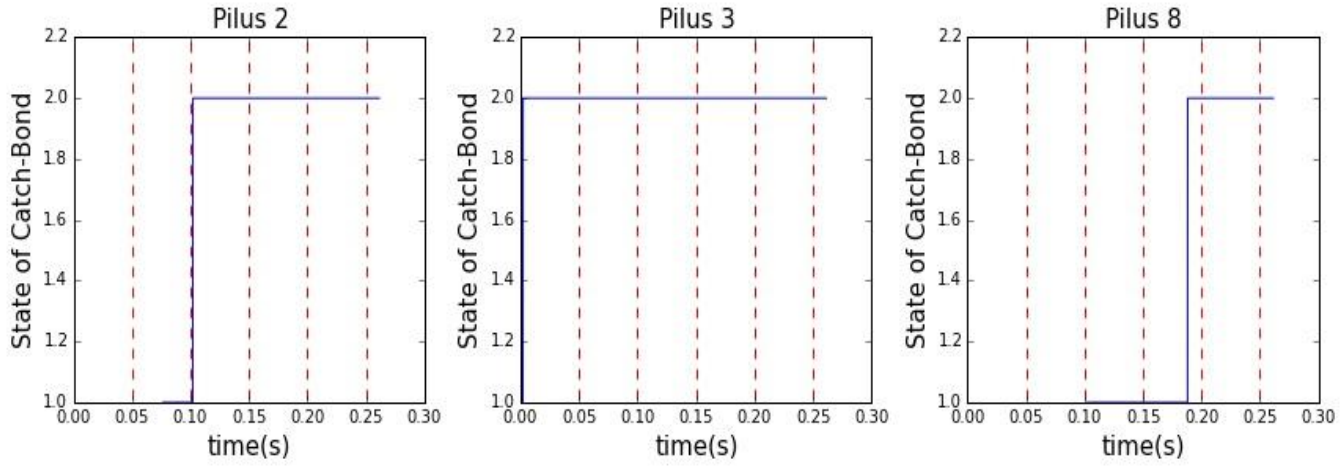

The pilus which anchors initially is the pilus 3 which enters extremely fast to the state, as time passes additional pilus begin to enter to this state providing of additional stable anchor points. The changes in shear are periodic between 7.5 pN/ (um) ^{2} and 0.25 pN/ (um) $^{2.}$

Figure 20. Time Evolution of the Pilus that present uncoiling

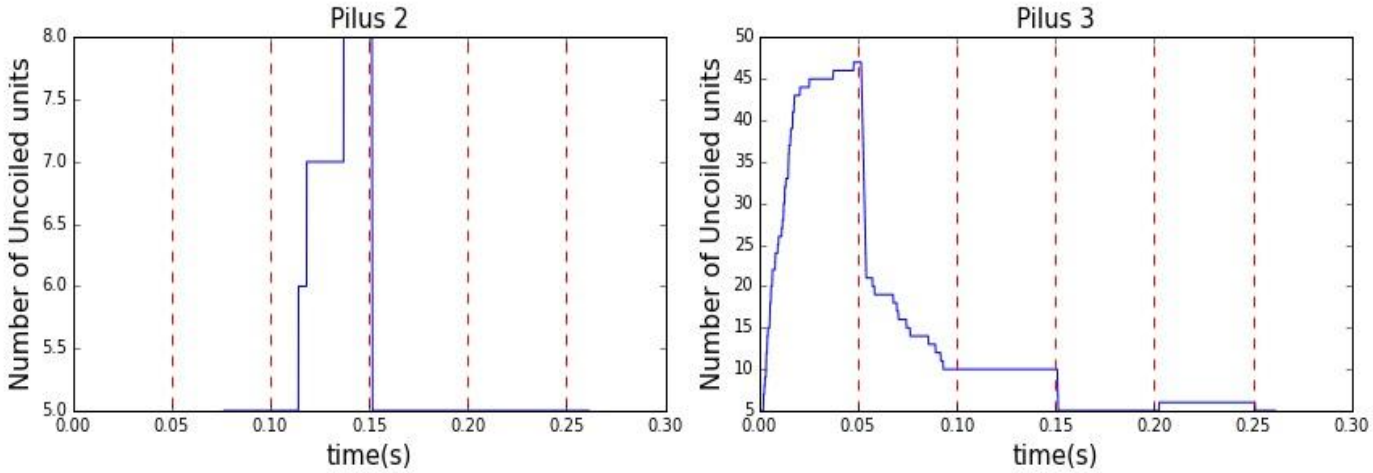

The pilus 3 quickly begins to unwind in the first cycle of high shear as it is the only pilus holding the bacterium. In the second cycle as pilus 2 and pilus 3 are the ones holding the system; the force is sheared between them so there is a smaller. The changes in shear are periodic between 7.5 pN/ (um) ^{2} and 0.25 pN/ (um) $^{2.}$r uncoiling. For the following cycle there are enough pilus attached to make the net force of the pilus small enough to not allow uncoiling.

Figure 21. Force response of individual pili over time

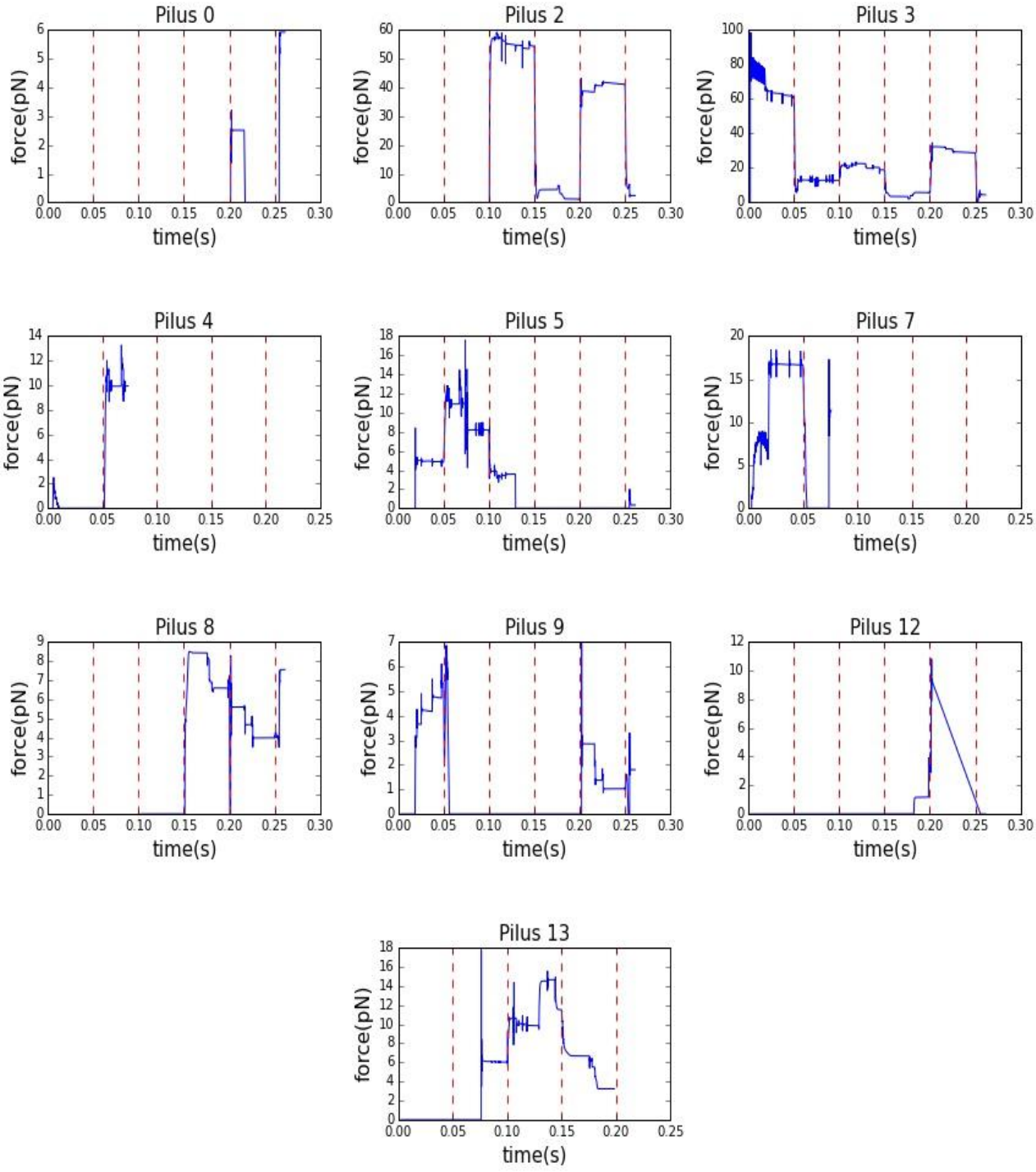

The leading pilus is the pilus 3. As time passes the load begins to be sheared by pilus 2,13 and 8. Indicating that more acochoring points are being created.

Figure 22 . Bacterium exposed to a period change in shear with rigidity

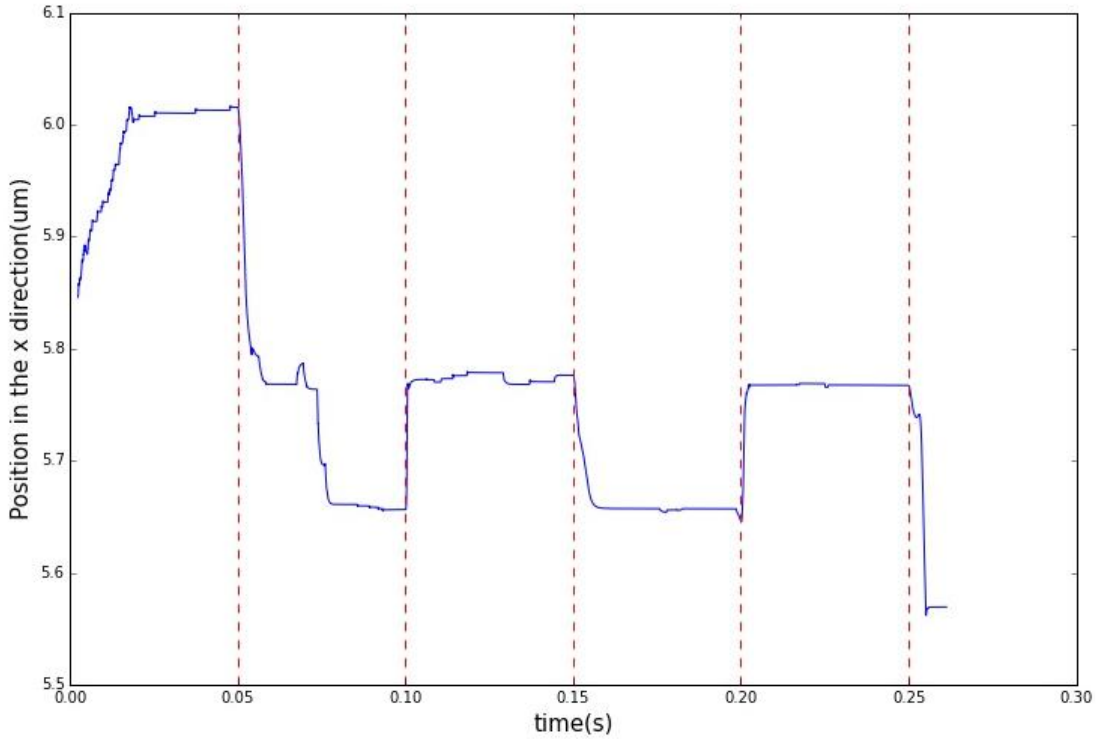

The same retracting behavior seen in Figure 16 appears again with the inclusion of rigidity but, the movement in clear damped by the pilus as it does not shows the sustained growth but rather a constant position.

An import thing that need to made clear is that there still need to further improve this model as, for some cases there are problems with the force that the pili made when compress, in particular in respect to the *dt.* In particular, when perform through long stretches there are error the force made by the buckling maybe too large (see Figure 23)

Figure 23. Problems with Buckling.

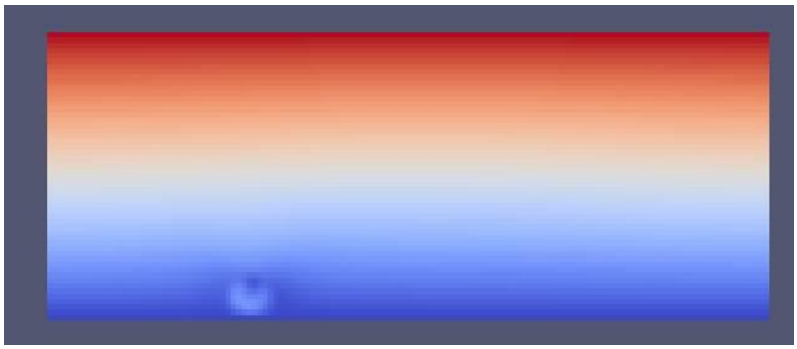

For more extended period of time the force made by the bucking becomes too large and begins to produce problems, it is necessary to make a study of dt with this element too. The color indicates velocity magnitude and the spot is the bacterium, it has an extremely large velocity compared to the domain. It seem that it bounces to strong from it collision with the pilus

Conclusions

The development of a computational model for the dynamic adhesion of a bacterium was successful, as the components that were required for the simulation (the fluid dynamics, non-linear force response of pili, and the stochastic adhesion) give in all validation test the expected behavior (both the pilus simulation and the catch-bond replicated experimental data and the fluid follow the expected analytics results for it). In what respects the integrated simulation, it was able to replicate some experimental behavior also seen for the whole system (the ability to move against the current). Overall, the creation of the model was achieved.

Each of the systems exists in a different time scale, (the one required for the stability of the fluid simulation, and those derived from the transition rated involved in the catch-bond and pilus deformation). To overcome this difficulty, it was necessary to find a way to adapt each time scale to the other. First, the necessary time scale for a stable fluid simulation and with a manageable

computation time was found. The characteristic time scale for the random transition for catch-bond and pilus was found by adding up the transition frequencies and getting their inverse.

It was noted that time the scale necessary for the fluid was too small for both the pilus simulation and the catch-bond simulation (there could be various fluid iteration before any transition could take place). The pilus relied on the use of Monte Carlo-Metropolis algorithm while the catch-bond on the Gillespie Algorithm, both of them deals differently with time so their adjustment for the time scale imposed by the fluid should be different. In this case, Monte Carlo-Metropolis the algorithm was only executed every hundred iterations of the fluid algorithm, and through this making it work in a more adequate time scale. In the case of the Gillespie algorithm, as the rates are force dependent, it was allowed that the normal evolution of the algorithm take place as long as the force that alters the rates remained constant.

The results of this simulation give insight on the underlining mechanics of dynamic adhesion. First, when an initial contact is made and the bacterium attaches to the surface, if the shear is high enough the pilus will produce a constant force that gets the catch-bond into it strong state quickly. It seems as a way to ensure an anchor point is fixed when it is needed. This behavior is noted first in the simulation when only one pilus is used. Then when considering various pili, this behavior also appears, and it can be noted that the first pili is the one that will receive the biggest load as the other pilus will take longer to attach and it is necessary for it to survive long enough so the other ones can attach. This fact can be noted in the Figure 21, initially pilus 3 receives the biggest load and in subsequent iteration more pilus get attach and reduce the load over it (in particular pilus 2).

Also another fact worth noting is the behavior of the retraction mechanism, which is an emergent phenomenon product of the presence of multiple pili. It can be seen in Figure 16; in each iteration the center of the bacterium displaces less in the direction of the flow direction, but at the

same time in Figure 17, there is an increase in pili attach so they damp the movement of the bacterium and reduces its displacement.

The importance of this work is that it allows a more detailed analysis of the dynamics behind the initial steps of infection. Additionally, it can be used to see which biological parameters hold a bigger influence over the capacity of attachment of the bacteria and by having information treatments can be develop with the purpose eliminating the infection, no through the use of antibiotics which kill the bacteria, but rather through medication that sabotages the particular parameter that make the attachment possible

References

[1] D. E. Rangel, N. Marín-Medina, J. E. Castro, A. González-Mancera, and M. Forero-Shelton, PLoS ONE **8**, e65563 (2013).

[2] M. Whitfield, T. Ghose, and W. Thomas, Biophys. J. **99**, 2470 (2010).

[3] J. Zakrisson, K. Wiklund, O. Axner, and M. Andersson, ArXiv Prepr. ArXiv14117586 (2014).

[4] G. I. Bell, Science **200**, 618 (1978).

[5] W. Thomas, M. Forero, O. Yakovenko, L. Nilsson, P. Vicini, E. Sokurenko, and V. Vogel, Biophys. J. **90**, 753 (2006).

[6] M. Andersson, O. Axner, F. Almqvist, B. E. Uhlin, and E. Fällman, Chemphyschem Eur. J. Chem. Phys. Phys. Chem. **9**, 221 (2008).

[7] O. Björnham, O. Axner, and M. Andersson, Eur. Biophys. J. **37**, 381 (2007).

[8] E. Miller, T. Garcia, S. Hultgren, and A. F. Oberhauser, Biophys. J. **91**, 3848 (2006).

[9] J. Zakrisson, K. Wiklund, O. Axner, and M. Andersson, Biophys. J. **104**, 2137 (2013).

[10] A. J. Goldman, R. G. Cox, and H. Brenner, Chem. Eng. Sci. **22**, 653 (1967).

[11] J. Howard, *Mechanics of Motor Proteins and the Cytoskeleton* (Sinauer Associates, Publishers, 2001).